Defect and Diffusion Forum Vols. 171-172 (1999) pp. 1-32
online at http://www.scientific.net

IR Studies of Oxygen-Vacancy Related Defects in Irradiated Silicon

C.A.Londos, L.G.Fytros, G.J.Georgiou

Solid State Section, Physics Department, Athens University,
Panepistimiopolis, Zografos, Athens 157 84, Greece

Keywords: Oxygen impurity, irradiation, infrared spectroscopy, localised vibrational mode

Abstract. The microscopic identification of a defect, i.e. its chemical nature, its physical structure and its geometrical configuration, is one of the most important aims of semiconductor research. In relation to that, a characteristic fingerprint of a defect is its corresponding Localised Vibrational Mode (LVM) signals in the IR spectra. Inversely, from the LVM frequency of a defect signal we get information for its structure. In this work, we mainly present infrared absorption measurements of irradiation-induced defects in Cz-grown Si. The work is primarily focused on oxygen vacancy-related defects formed in oxygen rich Si upon irradiation with subsequent thermal annealing. First, the structural properties of the various multivacancy-multioxygen (V_nO_m) defects, chiefly known from EPR studies, are reviewed. Certainly, direct correlations of LVMs bands with defects is a difficult task and theoretical calculations could provide guidance in interpreting experimental results. Thus, we subsequently report on systematic calculations of the vibrational frequencies of the centers VO_m (m=2,3,4), V_nO (n=2,3) and the [VO+O_i] defect. Among the larger complexes V_nO_m, we especially calculate the frequencies of the V_2O_2, V_3O_2 defects. We put forward a semiempirical model from which we estimate the frequencies of VO_m (m=2,3,4) defects. The frequencies of V_nO (n=2,3) defects result from the well-known valence force treatment model. The frequencies of V_2O_2, V_3O_2 complexes result from a semiempirical model employing dipole-dipole moment interactions. Next, the calculated values are discussed and compared with the values taken from other theoretical works. Finally, taking into account results from other experimental techniques cited in the literature, correlations are made of defect structures with LVM bands.

1. Introduction

Silicon is the most important semiconductor for the electronics technology. It is by far the most basic material due to its wide range of applications. The performance of Si devices is strongly influenced by the presence of lattice defects and impurities. Among the latter, oxygen is the most abundant and technologically important impurity, unintentionally added in the Si lattice during, growth. The silicon monocrystals are grown either with the Czochralski (Cz) [1,2] or the Floating-Zone (Fz) [1,2] technique. In Cz-grown material the oxygen concentration is on the order of $10^{18}cm^{-3}$ although in the Fz Si the concentration is of the order of 10^{15}-$10^{16}cm^{-3}$.

Oxygen in Si is significant both for technological and scientific purposes. Its presence has a lot of beneficial effects concerning electronics applications. Among them is the improvement of the mechanical strength [3] of silicon wafers, which is a very important property when they are used for integrated circuits, because the presence of oxygen inhibits plastic deformation during device processing. Another advantage is its role [4] in the internal gettering processes for removing unwanted metallic impurities in the silicon material. In this case, SiO_2 precipitates act as diffusion sinks for the metallic contaminant. Furthermore, the fact that oxygen does not introduce energy levels in the forbidden gap is very fortunate since its concentration is usually some orders of magnitude larger than the concentration of donor and acceptor atoms introduced to fabricate the

active region of integrated circuits. Of course, the presence of oxygen has also harmful effects especially in the case of uncontrolled oxygen precipitation in silicon. On the other hand, oxygen in Si presents a variety of optical, electrical and structural properties which have for a long time attracted scientific interest, helping in generally understanding the role of defects in semiconductors. Additionally, due to its high chemical activity oxygen has a very complex behaviour in silicon. It participates in numerous reaction processes which lead to a variety of complexes with lattice defects and impurities. Evidently, control of these defects, which is achieved by the detailed knowledge of their behaviour, is necessary for the improvement of the performance of Si devices. It is not, therefore, surprising that an extensive amount of theoretical and experimental work has been carried out concerning the various aspects of oxygen behaviour in Si. A lot of relevant review articles have been written [5,6,7,8]. However, despite a lot of research in the field, there are several issues that remain unresolved. Among them is the exact knowledge of the structure and properties of the numerous oxygen-related centers in Si. The study of these centers is the main purpose of this work.

There is a variety of ways by which defects can be introduced into the lattice [9]. One of the most common techniques for their introduction in the silicon matrix, in a controllable way, is by irradiation and subsequent heat treatment. All sorts of irradiation (electrons, neutrons, protons etc.) always lead to the formation of high concentration primary defects, i.e. self-interstitials and vacancies. The mechanism is the following:

When a particle with sufficient energy collides with a Si atom at a normal lattice site, the latter is kicked out at interstitial positions (Si_i) leaving a vacant site behind (V). At room temperature Si_i and V are very mobile and most of these species are annihilated by recombination ($Si_i + V \rightarrow \varnothing$). Nevertheless, a small percentage of these fundamental defects survives. Vacancies interact with each other to form divacancies [10,11] ($V + V \rightarrow V_2$). Self interstitials also pair together to form di-interstitials [12] $Si_i + Si_i \rightarrow Si_i - Si_i$. At room temperature these V_2 and Si_i - Si_i secondary defects are immobile. It is of interest to note that some of the divacancies could form directly during the collision process. In the case of neutron irradiation, large aggregates [13] of defects are also formed. These defect clusters mainly consist of a multivacancy "core" surrounded by an impurity complex "shell".

In spite of the above reactions, mainly concerning associations between lattice defects, reactions between lattice defects and impurities also take place readily. Oxygen is well-known [14,15] to be a very effective trap for irradiation-produced vacancies leading to the formation of the VO pair, (the so-called A-center), which is stable at room temperature (RT). The structure and properties of this defect and any other oxygen-related defects will be discussed later. Oxygen impurity also traps [16] silicon self-interstitials, leading to the formation of the O_i Si_i centers which are unstable at room temperature.

Upon heat treatment of Cz-grown irradiated Si, complexes involving oxygen impurities and lattice vacancies are formed. More specifically, upon annealing, families of multivacancy-multioxygen (V_nO_m) complexes form. Two main reaction channels are activated. The first one refers to the sequential reaction [16,17] $VO \xrightarrow{O_i} VO_2 \xrightarrow{O_i} VO_3 \xrightarrow{O_i} VO_4 \xrightarrow{O_i} \ldots$ where oxygen atoms are successively added, upon increasing the temperature, to the initial VO core. In essence, it is an oxygen agglomeration process. The members of this family have been studied in detail by EPR and Infrared Spectroscopy [17,18,19]. The second reaction channel refers to the sequential reaction [18] $VO \xrightarrow{V} V_2O \xrightarrow{V} V_3O \xrightarrow{V} V_4O \xrightarrow{V} \ldots$, where vacancies are added, upon increasing the temperature, to the initial VO defect. Thus, a vacancy agglomeration process also occurs at the same time. The members of this family have been studied in detail by the EPR and IR techniques [20,21]. Note, that due to the formation of divacancies, V_2O and V_3O defects could also form through reactions of the type $V_2 + O \rightarrow V_2O$, $V_2 + VO \rightarrow V_3O$, ... Other reactions also take place leading to the formation of larger complexes [20,22], especially in neutron irradiated Si, like V_2O_2, V_3O_2, V_4O_2,

V_3O_3 of the general type V_nO_m. Actually, in neutron-irradiated Si the number of multivacancies is expected to be larger. Thus V_3, V_4, V_5... defects also form. Their evolution with temperature is known [23]. Therefore, the concentrations of large V_nO_m defects are expected to be larger. These centers have been detected and investigated by a number of experimental techniques; for example Electron Paramagnetic Resonance (EPR) [20,24], Infrared Spectroscopy (IR) [17,21], Positron Annihilation Studies (PAS) [25,26] etc.

The electrical characterisation of the various V_nO_m defects is still incomplete and definite correlations of energy levels with certain defects have not yet been established. Tentative correlations, however, have been reported [27,28,29] in the literature.

Most of the oxygen-related defects are IR active, i.e. they have LVMs frequencies in the range of IR radiation. In general, the LVM frequencies of a defect are characteristic of the nature and geometry of this particular defect, and this explains why IR spectroscopy has evolved as a powerful technique for studying the structure and identity of defects. Its role is even more profound for the study of V_nO_m defects since, in general, as already mentioned, their associated energy levels in the gap and their electrical activity are not definitely known. In the field of IR spectroscopy the status of V_nO_m defects entails a lot of unanswered questions. The question of the definite attribution of the LVM signals in the IR spectra to certain defects has only been partially answered. The object of the present work is to establish certain correlations between LVM signals and the corresponding defect structures from which they originate. For this purpose, we have performed theoretical calculations of the vibration frequencies of the various V_nO_m defects, which, when combined with our experimental results, experimental data and theoretical works cited previously in the literature, they led to the following correlations: 839 cm^{-1} with V_2O defect, 914, 1000 cm^{-1} with [VO+ O_i] defect, 887 cm^{-1} with VO_2 defect, 833 cm^{-1} with V_3O_2 defect, 824 cm^{-1} with V_2O_2 defect, 884 cm^{-1} with V_3O defect, 899, 962, 993 cm^{-1} with VO_3 defect and 983, 1004 cm^{-1} with VO_4 defect.

The paper is organised as follows:

We shall first present the theoretical background of the electromagnetic interaction with the crystal matter and describe the physics of the Localised Vibration Modes which arise from impurities and defects in the crystal. Then, the fundamental aspects of the isolated oxygen, and the oxygen-related structures in Si will be presented. Later, we shall discuss the formation of the various V_nO_m defects in irradiated silicon and their properties will be reviewed. Experimental spectra from Infrared Spectroscopy will be given, and for every related structure we shall provide calculations of the corresponding vibrational frequencies. Finally, definite assignments will be attempted by combining our results with experimental results from various techniques and also theoretical results cited in the literature.

2. Theoretical background

2.1 Interaction of Electromagnetic radiation with matter

Upon examining the interaction between the incident electromagnetic radiation with the crystal, the Hamiltonian of the system (radiation-crystal) is normally taken as:

$$\hat{H} = \hat{H}_o + \hat{H}_{\text{int}} \tag{1}$$

where $\hat{H}_o$ is the term of the unpertubated crystal and $\hat{H}_{\text{int}}$ is the interaction term on which the present analysis will be focused. If the incident electromagnetic radiation is a polarised monochromatic wave described by the expression:

$$\vec{A}(\vec{r},t) = \vec{A}_o e^{i(\vec{k}\vec{r}-\omega t)} \tag{2}$$

where $\vec{A}(\vec{r},t)$ is the vector potential, following the procedure of "minimal substitution" $\hat{H}_{\text{int}}$ has finally the form [30]:

$$\hat{H}_{\text{int}} = \sum_i \vec{A}(\vec{r}_i,t)\frac{e}{mc}\hat{p}_i - \sum_j \vec{A}(\vec{r}_j,t)\frac{Z_j e}{M_j c}\hat{p}_j \tag{3}$$

where e and m are the absolute value of the electron charge and the mass respectively, $Z_j e$ and M_j the charge and the mass of the jth nucleus, respectively, and $\hat{p}$ the moment operator. The probability amplitude of the transition from an initial crystal state $|m\rangle$ to a final state $|n\rangle$ is given by the well-known relation [30]:

$$C_{mn} = \int_0^t \langle n|\hat{H}_{\text{int}}|m\rangle e^{i\omega_{mn}t'}dt' \tag{4}$$

where $\omega_{mn} = \omega_m - \omega_n$.

Upon substituting Eq.2 and Eq.3 to Eq.4, we obtain:

$$C_{mn}(t) = \int_0^t \langle n|\sum_i \vec{A}(\vec{r}_i,t)\frac{e}{mc}\hat{p}_i - \sum_j \vec{A}(\vec{r}_j,t)\frac{Z_j e}{M_j c}\hat{p}_j|m\rangle e^{i\omega_{mn}t'}dt' \quad \text{, or}$$

$$C_{mn}(t) = \int_0^t e^{i(\omega_{mn}-\omega)t'}\langle n|\sum_i \vec{A}(\vec{r}_i,t)\frac{e}{mc}\hat{p}_i - \sum_j \vec{A}(\vec{r}_j,t)\frac{Z_j e}{M_j c}\hat{p}_j|m\rangle dt' \tag{5}$$

In the case of infrared radiation, where the wave length is about 1000 times larger than the interatomic distance, we can assume that the spatial variation of the electric field is almost negligible. It is reasonable, therefore, to consider, for any electron or nucleus which belongs to a unit cell, the following approximation:

$$e^{ikr_i} \cong e^{ikR_l} \quad , \quad e^{ikr_j} \cong e^{ikR_l} \tag{6}$$

where R_l is the vector for the unit cell "l" of the crystal . Thus, Eq.4 finally becomes:

$$C_{mn}(t) = \int_0^t \left\{\langle n|\sum_i \frac{i\omega e}{c}\vec{A}_o e^{i(kR_l-\omega t)}\hat{r}_i - \sum_j \frac{i\omega Z_j e}{c}\vec{A}_o e^{i(kR_l-\omega t)}\hat{r}_j|m\rangle e^{i\omega_{mn}t'}\right\}dt' \tag{7}$$

Noting that a plane wave in the Coulomb gauge has the form:

$$\vec{E} = \frac{i\omega}{c}\vec{A}_o e^{i(kR_l-\omega t)} \tag{8}$$

and setting

$$\vec{\mu} \equiv -\sum_i e\vec{r}_i e^{ikR_l} + \sum_j Z_j e\vec{r}_j e^{ikR_l} \tag{9}$$

we find the probability amplitude:

$$C_{mn}(t) = \int_0^t \langle n|-\vec{E}\cdot\vec{\mu}|m\rangle e^{i\omega_{mn}t'}dt' \tag{10}$$

According to the theory of lattice vibrations in solids, and especially in the case of a crystal with two atoms in the unit cell, there are two branches of allowed frequencies: the acoustical branch and the optical branch. For frequencies in the optical branch the corresponding motion of the atoms induces a varying dipole moment. Thus, for frequencies in the optical branch and especially for small values of k, $(k \to 0)$, a strong coupling with the electromagnetic field is achieved. These frequencies lie in the infrared range of the spectrum. The term e^{ikR_l} in Eq.9 therefore could be taken approximately equal to unity leading to the relation:

$$\vec{\mu} \equiv \left(-\sum_i e\vec{r}_i + \sum_j Z_j e\vec{r}_j \right) \tag{11}$$

which provides the dipole moment of the unit cell [31].
The corresponding operator for the dipole moment can be written as an expansion of linear and generally multilinear terms [31] as follows:

$$\hat{\mu} = \hat{\mu}_o + \sum_{l,a} e^{ikR_l} \hat{\mu}\begin{pmatrix} l \\ a \end{pmatrix} u_a(l) + \sum_{\substack{l,a \\ l',b}} e^{ikR_l} \hat{\mu}\begin{pmatrix} l & l' \\ a & b \end{pmatrix} u_a(l) u_b(l') + \cdots \tag{12}$$

Substituting Eq.12 into Eq.10 we have:

$$C_{mn}(t) = \int_0^t \langle n| - \vec{E} \cdot \left\{ \hat{\mu}_o + \sum_{l,a} e^{ikR_l} \hat{\mu}\begin{pmatrix} l \\ a \end{pmatrix} u_a(l) + \sum_{\substack{l,a \\ l',b}} e^{ikR_l} \hat{\mu}\begin{pmatrix} l & l' \\ a & b \end{pmatrix} u_a(l) u_b(l') + \cdots \right\} |m\rangle e^{i\omega_{mn}t'} dt' \tag{13}$$

The first term, $\hat{\mu}_o$, in Eq.13 clearly vanishes since the eigenfunctions of the vibrational states are orthonormals.

The second term, $\sum_{l,a} e^{ikR_l} \hat{\mu}\begin{pmatrix} l \\ a \end{pmatrix} u_a(l)$, describes [32] the transition from $n = 0$ to $n = 1$, specifying a process where one photon is absorbed and one phonon is activated (one phonon process) . Note that at room temperature almost all the defects are found in the fundamental state. A small percentage of them occupy higher energetic states, but the allowed transitions fulfil the rule $\Delta n = 1$. The quantity $\hat{\mu}\begin{pmatrix} a \\ l \end{pmatrix}$ has the dimensions of charge and is generally called "apparent charge" or "effective charge" denoted by the letter "η". This term is dominant [33] in ionic crystals but vanishes in diamond type crystals like Si or Ge. In the latter crystals there are two identical atoms in the unit cell and one point of inversion symmetry. Due to the fact that the two atoms have equal but opposite displacements the induced dipole moment is zero. However, if an impurity or a defect is present, the inversion symmetry is locally destroyed, the dipole moment varies and, therefore, one phonon processes become dominant for the absorption. Note that, in general, the apparent charge of defects is very difficult to estimate, since the electron distribution of the atoms involved is almost impossible to describe accurately.

The third term, $\sum_{\substack{l,a \\ l',b}} e^{ikR_l} \hat{\mu}\begin{pmatrix} l & l' \\ a & b \end{pmatrix} u_a(l) u_b(l')$, describes [32] the transitions from $n = 0$ to $n = 2$, and generally transitions where $\Delta n = 2$, specifying a process where one photon is absorbed and two phonons are activated (two phonon process). In the case of a homopolar crystal like Si this is the dominant term for the absorption process. From the two phonons that are activated, the first one induces a charge on the atoms and the second causes the vibration of these atoms, thus producing a varying dipole moment which leads to absorption. When impurities are incorporated in the host lattice, or, more generally, when various defects are present, the study of the absorption is more complicated, since the number of the constituents involved increases and the expected number of normal modes is therefore larger. In any event, it is important to determine how the dipole moment varies with the displacement of the defect constituents and the neighbouring host lattice atoms. Note that, the two phonon process depends upon temperature, and more specifically, when the temperature decreases the corresponding intensity of the absorption also decreases. In contrast, the one phonon process is not characterised by a similar behaviour. The two phonon process leads to an inherent background absorption characteristic of the crystal, and in the case of studying defect signals, it should be removed.

Generally the notion of the apparent charge is replaced by that of an "apparent charge tensor" [32] given by the expression :

$$\eta_{nj:x} = \frac{\partial \mu_x}{\partial u_{nj}} \quad , \quad j = x, y, z \tag{14}$$

where u_{nj} is the displacement at the nth atom and M_x is the x-component of the dipole moment.

2.2 Localised Vibrational Modes of points defects

It is well known that in a perfect crystal [32] there are ranges of allowed frequencies, which means that disturbances with frequencies within these ranges propagate into the crystal. Such disturbances are described by a travelling wave,

$$u_n = A\, e^{i(qx_n - \omega t)} \tag{15}$$

where x_n is the displacement of the nth atom. Disturbances with frequencies outside these regions cannot propagate.

If any of the host crystal atoms is substituted by an impurity, or, generally, by a defect, then the periodicity of the crystal is destroyed. As a consequence, new normal modes appear with corresponding frequencies either in the forbidden gap or within the allowed range [32]. Due to the impurity, the charge density is locally polarised and an additional dipole moment is induced. Because of this extra dipole moment coupling with the electromagnetic radiation becomes possible and the one phonon process dominates in the absorption. This additional absorption is significant, especially in the range of frequencies corresponding to the normal modes arising in turn from the impurity. The corresponding vibration cannot propagate in the crystal. Its amplitude decreases exponentially and in essence vanishes in the range of a few neighbouring atoms from the impurity. The vibration is localised in the range around the impurity location and is called "Localised Vibrational Mode" (LVM). Excellent reviews on this topic exist in the literature [32,33].

If the mass of the impurity is smaller than the mass of the host atom, the frequency of the LVM is larger than $\omega_{\max}$, where $\omega_{\max}$ is the maximum allowed frequency in the perfect crystal. The corresponding disturbance is described by [34]:

$$u_n = A(-1)^{|n|}\, e^{|n| \ln B} \tag{16}$$

where B is a constant which depends on the masses M and M_o of the impurity and host atoms respectively. The LVM frequency depends upon the mass of the impurity and the modified force constant K of the bond [34]. It is given by the relation,

$$\omega_{LVM} = \frac{\omega_M}{\sqrt{1-\varepsilon^2}} \tag{17}$$

where $\omega_M = 2\sqrt{K/M_o}$ and $\varepsilon = 1 - \frac{M}{M_o}$. It is obvious that $\omega_{LVM} \rangle \omega_{\max}$. Note that, the smaller the ratio M/M_o, the more localised is the induced vibrational mode. The FWHM (Full width at half maximum) of the LVM band becomes smaller with decreasing temperature but the height of the peak does not depend on the temperature. Evidently, if one in addition recalls that two phonon absorption is reduced with temperature, measurements at low temperatures are preferable because a superior signal/ noise ratio and a higher resolution can be achieved.

The integrated absorption of a LVM is related directly to the concentration of the impurity and is given by the relation [32]

$$\int a d\omega = \frac{2\pi^2 \eta^2 N}{nMc} \tag{18}$$

where n is the diffraction index of the crystal, C is the speed of light, η is the apparent charge, M the mass of the impurity and N its concentration. The apparent charge due to the impurity and the corresponding concentration are generally not known. Determination of the above parameters, especially the concentration (which is important for technology), necessitates calibration. Thus, a calibration factor denoted by K^* is introduced, so that $\int a d\omega = K^* N$. This factor is determined by independed experiments using crystals where the concentration, N, of the impurity is known. For room temperature measurements, a recent, widely used value [7] for the calibration factor of the oxygen impurity in Si is $3.14 \times 10^{17} \times a_o \, \mathrm{cm}^{-1}$, where a_o is the peak absorption coefficient of the 9μm band of oxygen. For low temperature measurements different calibration factors have been proposed [2]. It is important to note that there is a lower limit [32] for the concentration of the impurities, which is approximately, $N_{imp} \approx 10^{16} \, cm^{-3}$. This means that impurities with smaller concentrations cannot be detected by Infrared Spectroscopy.

3. Oxygen in Silicon

3.1. Oxygen interstitial

A prerequisite for understanding V_nO_m defects in Si is to firstly know the behaviour of the oxygen impurity. Oxygen atoms in the silicon matrix occupy interstitial sites [35]. X-ray diffraction measurements [36] have shown that the presence of oxygen increases the average lattice parameter, a safe indication of interstitial incorporation. In particular, oxygen occupies an off-center bond-centered (BC) interstitial site [6]. Analysis of IR spectroscopy data indicates that it is bonded to two Si atoms (Fig.1) forming a non-linear Si-O-Si pseudomolecule with C_{2v} symmetry. The oxygen atom

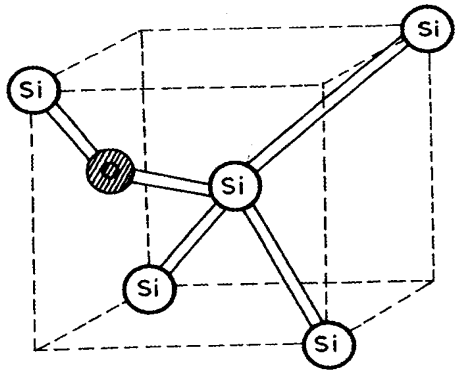

Fig. 1: The configuration of the O_i center.

is displaced [37] by 0.022nm from the <111> Si-Si axis, the angle between the Si-O bonds being about 162° and the Si-O bond length [38] about 0.161nm. Its accommodation in the silicon lattice is achieved by breaking the covalent bond between two neighbouring Si atoms. Energetically [39] this is not prohibited since the energy of the Si-Si bond in silicon is 2.3 eV, whereas the energy of Si-O bond in the SiO_2 is 4.8eV, and one Si-Si bond is replaced by two Si-O bonds. The interstitial position of oxygen in silicon is generally accepted. However, O'Mara [8,40] taking as a basis IR results by

Bosomworth et al [37] has suggested that part of the oxygen atoms occupy substitutional sites in the silicon lattice. The weak point [7] of this supposition, which may be consistent with some experimental data, is that the four valence bond configuration for oxygen in this position is very unlikely. Early infrared studies [41] of the vibrational behaviour of oxygen in Si have associated three frequencies to the oxygen impurity. The Si-O-Si molecule gives rise to a frequency i) at 1106 cm^{-1} attributed to the antisymmetric stretching mode, ii) at 515 cm^{-1} attributed to a symmetric bending mode and iii) at 1206 cm^{-1} attributed to a symmetric mode. It is noted that the 515 cm^{-1} mode is in the band mode region and therefore is considered as an in-band oxygen-induced resonance [42,43]. Thus, it cannot be treated [32] as a simple molecular vibration. Also the 1206 cm^{-1} mode should be related to a combination of the antisymmetric stretching mode with the libration of the oxygen atom about the <111> axis which contains the two silicon atoms. Low oxygen-related modes [37] at 29 cm^{-1} have been attributed to the vibration of the oxygen atom in the (111) plane perpendicular to the Si-Si broken bond. In general, oxygen impurity is the origin of a number of infrared absorption bands [44] in the range of 27-1750 cm^{-1}.

Theoretically, oxygen in Si was initially treated [6,37,45] as a foreign atom that breaks a Si-Si bond, establishing in this way a non-linear quasimolecule with C_{2v} symmetry. Despite the merits of the above analysis, recent calculations have shown [46,47,48] that a better description of the oxygen related infrared spectra could be achieved by considering a linear pseudomolecule $Si_3 \equiv Si - O \equiv Si_3$ with a D_{3d} symmetry. Within the framework of the latter model most of the experimental results fall in place and a better understanding of oxygen impurity in Si is achieved.

No electrical activity of the oxygen interstitial in Si has been observed. Note that O is a group VI element and that other elements of the same group like S, Se, Te, are double donors [49]. However, the electrical activity of the latter is explained by their substitutional position in the silicon lattice, which is not favourable for oxygen due to the small tetrahedral radius of the oxygen atom. Theoretical analysis [50] of the SiO_2 structure shows that the corresponding molecular orbital in an infinite Si lattice is below the top of the valence band and does not give donor levels in the energy gap of Si.

3.2 Oxygen-related donors (Thermal Donors)

Note that Cz-Si indeed shows an electrical activity [51,52] coming from a series of donors, the well-known TDs which are related to oxygen [53,54]. The exact structure of TDs remains an unresolved issue despite many efforts in the last forty years, and the progress that has been achieved so far. It is well-known [53] however, that TDs are not unique defects and consist of a series of as many as 16 centers formed consecutively upon heat treatment in the temperature range of 400-500°C. FTIR spectroscopy studies of the Rydberg states of these donors have revealed the presence of double donors states labelled TD_1, TD_2,...,TD_{16} appearing successively in the spectra upon annealing. General consensus has it that oxygen participates in their structure. Although, TDs are of no concern in the present work, it is worth noting, that LVMs attributed to them have been observed very recently [55]. Thus absorption bands at 975, 988, 1000, 1006 and 1012cm^{-1} were reported to be related to TDs.

TDs are destroyed with a short time heat treatment at 650°C. After their destruction the electrical activity of Cz-grown Si is the same as that of Fz silicon with the same dopant concentration. The latter observation confirms that interstitial oxygen is electrically inactive.

3.3 Oxygen dimers

Experimental data concerning oxygen diffusion in Si, as well as the formation process of thermal donors, assume [56,57] the existence of fast diffusing oxygen dimers. Two types of oxygen dimers have been suggested [56,58]. The first one consists of a pair of two adjacent oxygen atoms $(O_i + O_i \leftrightarrow O_2)$ forming an oxygen molecule, which cannot be stable. Indeed, these oxygen molecules are highly mobile since they do not possess a Si-O bond and they are only loosely coupled to the Si lattice. The second one consists [59] of two oxygen interstitial atoms at adjacent Si bonds with a common apex (Fig.2), forming a dimmer complex which is bonded to the Si lattice and it can

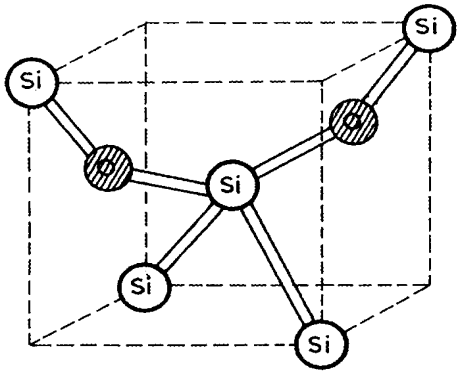

Fig. 2: The configuration of oxygen dimer.

be stable at a certain configuration. Oxygen dimers are appreciably more mobile [60] defects than oxygen interstitials and their existence could account for a lot of observations concerning oxygen diffusion, oxygen aggregation processes and TDs formation in Si. Recent IR absorption studies have verified their presence and three LVMs at 1012, 1060 and 1105 cm^{-1} were attributed [61] to them. Considering the formation of V_nO_m complexes, the participation of oxygen dimers in this process at elevated temperatures may be an interesting idea worthy of consideration.

3.4 Precipitated Oxygen

Heat treatments at temperatures generally higher than 650°C lead to oxygen precipitation; that is, to the growth of SiO_2 particles (oxide precipitates). IR spectroscopy studies reveal that oxygen precipitates give rise [2,7] to a broad absorption band at ~1226cm^{-1} and another band at ~1120cm^{-1}, which underlies the 9μm band from oxygen interstitial. There are [62] different shapes, phases and morphologies and kinds of oxygen precipitates. Their formation depends upon various factors among them the annealing temperature, the thermal history of the samples and their concentration in oxygen and carbon. Thus annealing in the range of 400-750°C gives rise to a broad peak in the range 1030-1100 cm^{-1} which has been attributed to amorphous SiO_x (x<2). Annealing in the temperature range of 750-950°C gives rise to a double peak at 1125 and 1222cm^{-1} which has been attributed to a-quartz or a-cristobalite. The latter attribution cannot be considered as conclusive since the presence of cristobalite has not been confirmed. In addition, the 1222 cm^{-1} band has been also attributed to platelet-shaped precipitates [63]. Two peaks at 1100 and 472 cm^{-1} that show up upon annealing in the temperature range of 950-1100°C were ascribed to amorphous SiO_2. In any case, the whole picture concerning oxygen precipitates, their formation kinetics and the underlying

mechanisms is not totally clear so far. The exact correlation between the various LVM bands and certain precipitates is pending further investigation.

4. VO_m defects

In this section we shall study defects formed by an oxygen agglomeration process where oxygen atoms are sequentially added to an initial VO core. Their general form is VO_m and the main representatives of this group are the VO_2, VO_3 and VO_4 defects. For a comprehensive understanding of them, and for the purpose of estimating their corresponding LVMs, it is necessary to first study the VO defect.

4.1 VO center

As already mentioned, oxygen atoms are very effective traps for irradiation-introduced vacancies readily leading to the formation of the vacancy oxygen (VO) pair. This defect, usually known as A-center, is one of the most extensively studied defect, not only in silicon, but in all semiconductors where oxygen appears. EPR and optical studies [14,15,17,64,65] have provided its microscopic identification and suggested an atomic model where the oxygen atom is located in an off-center substitutional site in the <100> direction. Therefore, it could be considered as a nearly substitutional oxygen (Fig.3). Alternatively, the center can be considered as a vacancy where one of the reconstructed bonds is decorated by an oxygen atom [6]. In the neutral charge state it gives rise to an IR band at 830 cm^{-1} . The negative charge state of the defect gives rise to an IR band at 885 cm^{-1} [66].

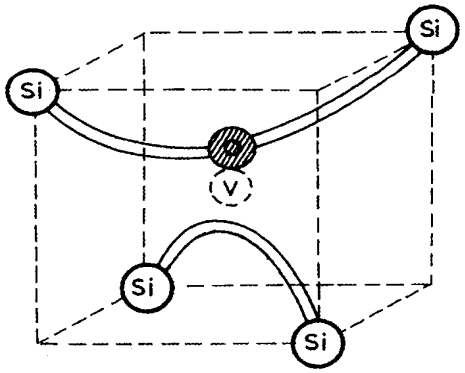

Fig. 3: The configuration of VO center.

The A-center has a negative paramagnetic charge state (VO^-) responsible [14] for an EPR spectrum labelled (Si-B1), and a neutral diamagnetic charge state (VO^o). Upon optical excitation the latter state becomes visible by EPR, giving rise [67] to the (Si-B1) spectrum. The center exhibits a rhombohedral symmetry with the dipole moment along the <110> axis.

The negative charge state VO^- is responsible for an acceptor level at E_c-0.17eV [68]. The emission of the trapped electron gives a Deep Level Transient Spectroscopy (DLTS) peak [69] with an activation energy of 0.18eV. The origin of the electrical activity of VO center arises [6] from the

fact that the reconstructive Si-Si bond is made up of two dangling bonds, with one bonding state filled with two electrons and one empty antibonding state.

Considering the VO center as an isolated pheudomolecular unit we can use the valence force treatment method [70]. According to this method, the VO center, which has a C_{2v} symmetry, has three infrared active modes, where only one, called ν_3, is observed clearly in the IR spectra [71]. The frequency of this vibrational mode is given by the formula:

$$(2\pi\nu_3)^2 = \left[1+\left(\frac{2M_{Si}}{M_O}\right)\sin^2 a\right]\frac{K_1}{M_{Si}} \qquad (19)$$

where M_{Si} and M_{Si} are the masses of the silicon and oxygen respectively, $2a$ is the angle between the two Si-O bonds and K_1 the force constant of the bond Si-O. From the above relation finally we take that the frequency is ν_3=830 cm^{-1}.

The presence of oxygen in the center is verified by the effect of isotopic oxygen doping [15] on the vibrational frequency of the localised mode; it is also verified by the reduction in the strength of the 1106 cm^{-1} band of oxygen interstitial when the 830 cm^{-1} band is formed. Optical measurements [72,73] showed an approximate one to one correspondence between the loss of the former band and the increase of the latter. The presence of vacancies in the A-center was confirmed [74] by the irradiation of heavily tin(Sn) doped-Cz-Silicon. Stress- induced dichroism measurements have shown a reduction in the rate of formation of the A-center by a factor of ~6 compared to undoped Cz-Si. The reason is that Sn traps mobile vacancies very efficiently, and therefore competes with oxygen, leading to the reduction of A-centers.

4.2 VO_2 center

At about 300°C the A-center anneals out. The decay of the 830 cm^{-1} band is accompanied by the emergence of a band at 887 cm^{-1} (Fig.4), attributed [17] to the VO_2 center. The annealing behaviour of the VO center is not completely understood [75,76], since VO may participate simultaneously in more than one reaction channels. The main reaction process is, however, $VO + O_i \rightarrow VO_2$, where diffusing VO pairs are captured by oxygen interstitial atoms leading to the formation of VO_2 defect. In the suggested structure of VO_2 defect two oxygen atoms equivalently share a vacancy site (Fig.5). The presence of two oxygen atoms is also supported [77] by the fact that the amplitude of 887 cm^{-1} band, as measured when VO signal, has completely annealed out, displays a quadratic dependence on the initial oxygen concentration of the silicon material. In the VO geometry the oxygen pair is orientated along the <100> axis and the defect has a D_{2d} symmetry. However, there is experimental data [6,78] that is not in agreement with the assignment of 887 cm^{-1} band with VO_2 defect. The main points that cast doubt about the origin of 887 cm^{-1} band are the following:

i) Uniaxial stress data [37] on this band suggest a C_{1h} defect symmetry which is lower than the D_{2d} symmetry of the VO_2 structure, ii) Implantation of Cz-Si with equal doses of ^{16}O and ^{18}O has failed to produce upon annealing the expected $^{16}OO^{18}V$ LVMs, which is a strong indication [79] against the presence of two oxygen atoms in the defect structure, unless the two atoms are weakly coupled. Theoretical studies [80], however, have shown that oxygen atoms are sufficiently far apart and interact only weakly. iii) During the emergence of the 887 cm^{-1} band there is no loss [76,81] of O_i atoms, as indicated by the stable amplitude of the 1106 cm^{-1} of oxygen interstitial. Note, in addition, that the structure of the VO_2 defect has not been completely verified by any microscopic experimental technique. All these have left the ground open for alternative suggestions . Thus, different geometrical structures, as for example the Si_3O_2 complex [82], have been put forward as candidates, and correlations of the 887 cm^{-1} band with other defects, for example the V_3O complex

[18], which has also appeared in the literature. The latter correlation is important in explaining uniaxial stress experimental data and will be discussed further latter, when we shall calculate the vibrational frequency of the V_3O defect.

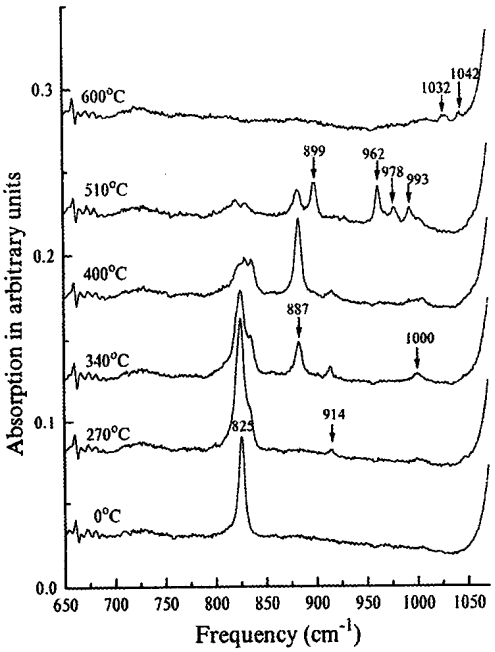

Fig. 4: IR spectra of neutron irradiated Si annealing at various temperatures. (ref.[19])

The electrical activity of the VO_2 defect remains an unresolved issue. Calculations show [80,83] that there are no energy levels in the forbidden gap associated with the defect. The pair of the two oxygen atoms passivates [80,84] the electrical activity of the lattice vacancy into which it is

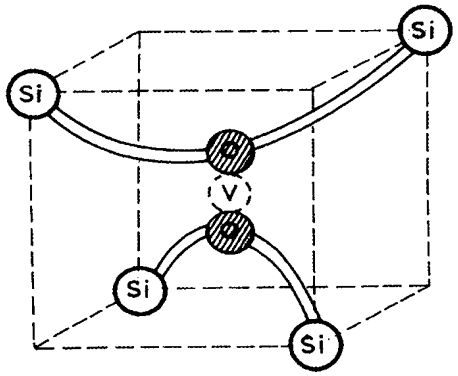

Fig. 5: The configuration of VO_2 center.

inserted. Thus, an acceptor state like that of VO is not expected. Also, since the oxygen atoms are

far apart, they are not expected to display a donor behaviour. It has been argued, however [80], that the presence of surrounding interstitial oxygen atoms could enable the VO_2 structure to exhibit a shallow double donor behaviour which is characteristic of thermal donors. For this reason, the VO_2 defect has been considered as a candidate for the core of thermal donors. However, resistivity measurements have shown [85] that the VO_2 defect has no electrical activity and it is not involved in the generation of thermal donors. In any case, and for the sake of completion, we report that energetic levels, for example the E_c-0.11eV level [86], have been tentatively attributed to the VO_2 defect. We note, in addition, that the VO and VO_2 defects are also detected by Positron Annihilation Studies (PAS) and bulk lifetimes of 270ps and 240ps have been, respectively, correlated [87] with the above defects.

In order to calculate the LVM frequency of the VO_2 defect it seems to be more instructive to begin with the study of the geometry of the VO center and then to evaluate the changes that occur by introducing an additional oxygen atom at the same vacancy site. The geometry is depicted in the (Fig.6). Thus, according to the theory of the covalent bond, we assume that the oxygen atom is subjected to a power low potential [88,89]:

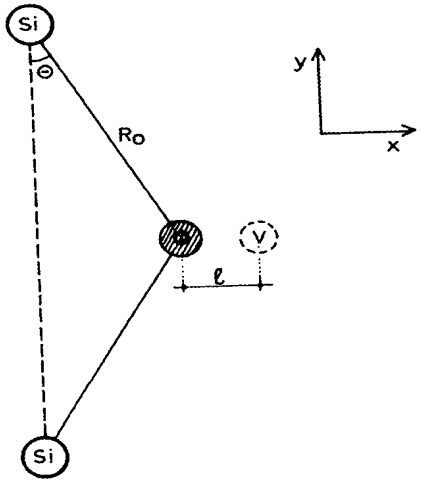

Fig. 6: The VO geometry depicted in the <110> plane.

$$U(r) = \varepsilon\left[\left(\frac{\sigma}{R}\right)^4 - \left(\frac{\sigma}{R}\right)^2\right] \tag{20}$$

where ε and σ are empirical constants and R is the length of the Si-O bond. The vibrational frequency of 830 cm^{-1} arises from the stretching mode of the oxygen atom in the y-direction. Since the oxygen atom is bonded with two Si atoms the total potential, for small displacements around the equilibrium site, is given by the expression:

$$U_{tot} = \varepsilon\left[\left(\frac{\sigma}{R + y\cos\vartheta}\right)^4 - \left(\frac{\sigma}{R + y\cos\vartheta}\right)^2 + \left(\frac{\sigma}{R - y\cos\vartheta}\right)^4 - \left(\frac{\sigma}{R - y\cos\vartheta}\right)^2\right] \tag{21}$$

Upon expanding this relation in a Taylor series and keeping only second order terms we find:

$$U_{tot} = \varepsilon\frac{\sigma^2}{R^4}\left(20\left(\frac{\sigma}{R}\right)^2 - 6\right)y^2\cos^2\vartheta \tag{22}$$

Given the validity of Hook's law, the potential energy has the general expression:

$$U_{tot} = \tfrac{1}{2} K y^2 \tag{23}$$

where K is the force constant. Combining Eqs.22 and 23 we have:

$$K = 2\varepsilon \frac{\sigma^2}{R^4}\left(20\left(\frac{\sigma}{R}\right)^2 - 6\right)\cos^2\vartheta \tag{24}$$

Minimising the potential energy given by Eq.20, the length R_o of the Si-O bond at the equilibrium position is found to be $R_o = \sqrt{2}\sigma$. The corresponding value of the force constant is then

$$K = 8\varepsilon \frac{\sigma^2}{R_o^4}\cos^2\vartheta \tag{25}$$

Upon introducing the second oxygen atom, a new situation is established. In order to study the new structure we shall consider the initial oxygen atom under the influence of the dipole field of the added oxygen atom (Fig.7). The effective charge of the added atom has a value $\eta = 1.02|e|$ [90] leading to a dipole moment,

$$\vec{\mu} = -\eta(a - x)\hat{r} \tag{26}$$

where $\hat{r}$ is the unit vector from O_2 towards O_1, which due to the two equivalent Si-O bonds lies on

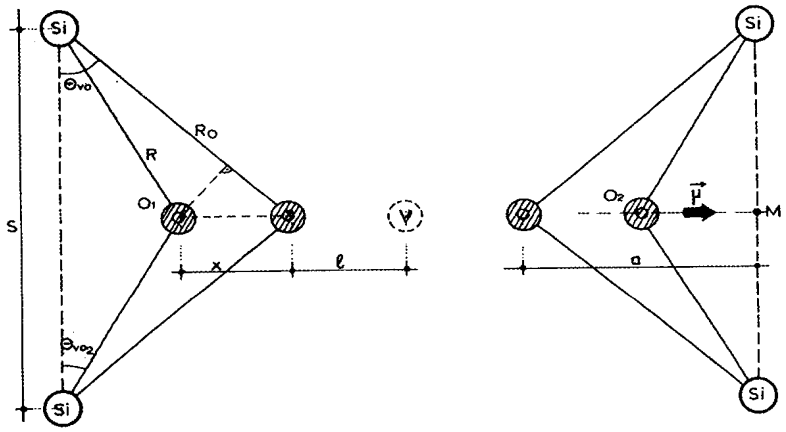

Fig. 7: The geometry of the VO center with an additional oxygen atom attached at the same vacant site.

the x-axis, as depicted in the (Fig.6). We assume that this dipole moment lies in the middle of the O_2M segment. The corresponding electric field is given by the familiar expression for dipoles,

$$\vec{E} = \frac{1}{4\pi\varepsilon_o}\frac{3\hat{r}(\vec{\mu}\hat{r}) - \vec{\mu}}{r^3} \tag{27}$$

Under the influence of this field the initial oxygen atom is pushed towards the Si atoms to which it is bonded and its new equilibrium position is characterised by the relation

$$E\eta = K'x \tag{28}$$

where K' is the force constant in the direction of the x-axis and x is the displacement of the initial oxygen atom due to the addition of the second oxygen atom.
Combining Eqs.26, 27 and 28 we finally get:

$$K'x = \frac{2\eta(a - x)}{4\pi\varepsilon_o(a + 2l + x)^3}\eta \tag{29}$$

K' has the value of 92,16 $\frac{Kgr}{\sec^2}$ [80]. Taking into account that $R_o = 1.66\text{Å}$ and $\vartheta = 18^o$ [91] we easily evaluate $a = R_o \sin\vartheta = 0.5129\text{Å}$. On substituting these values into Eq.29 we get the value of the x displacement, $x = 0.08058\text{Å}$

It is worthy of note that the oxygen atoms in both the VO and VO_2 structures vibrate in the y-axis. Thus, from Eq.24, the ratio of the force constants K_{VO} and K_{VO_2} of the VO and VO_2 structures, is

$$\frac{K_{VO}}{K_{VO_2}} = \frac{8\varepsilon\frac{\sigma^2}{R_o^4}\cos^2\vartheta_{VO}}{2\varepsilon\frac{\sigma^2}{R^4}\left(20\left(\frac{\sigma}{R}\right)^2-6\right)\cos^2\vartheta_{VO_2}} \tag{30}$$

where R is the distance between the Si and O atoms in the VO_2 configuration, which leads to

$$K_{VO_2} = K_{VO}\frac{\left(20\left(\frac{\sigma}{R}\right)^2-6\right)\cos^2\vartheta_{VO_2}}{4\cos^2\vartheta_{VO}}\left(\frac{R_o}{R}\right)^4 \tag{31}$$

Since, in general, $K = m\omega^2$ one has

$$\omega_{VO_2} = \omega_{VO}\left(\frac{R_o}{R}\right)^2\frac{\cos\vartheta_{VO_2}}{\cos\vartheta_{VO}}\frac{1}{2}\left(20\left(\frac{\sigma}{R}\right)^2-6\right)^{\frac{1}{2}} \tag{32}$$

As is easily seen from Fig.6

$$\cos\vartheta_{VO} = \frac{s/2}{R_o} \quad \text{and} \quad \cos\vartheta_{VO_2} = \frac{s/2}{R} \tag{33}$$

In view of Eqs.32 and 33 we obtain:

$$\omega_{VO_2} = \omega_{VO}\left(\frac{R_o}{R}\right)^3\frac{1}{2}\left(20\left(\frac{\sigma}{R}\right)^2-6\right)^{\frac{1}{2}} \tag{34}$$

Assuming now that the displacement of the silicon atoms that are bonded to the oxygen impurity is negligible, we can write:

$$R = R_o - x\sin\vartheta \tag{35}$$

whereupon we get $R \approx 1.635$ Å. Since $\sigma = \frac{R_o}{\sqrt{2}} = 1.1738$ Å, by substituting in Eq.34 we finally have:

$$\omega_{VO_2} \approx 898cm^{-1}$$

Indeed, this calculated value is very close to the experimentally observed frequency of $887cm^{-1}$ for VO_2 defect.

4.3 [VO+O_i] center

An important characteristic of the transformation process of the VO defect to the VO_2 defect through the reaction $VO + O_i \rightarrow VO_2$, is the formation of an intermediate defect structure [19,92]. As such a defect, a [VO+O_i] geometry has been suggested [19], where an oxygen interstitial atom and a VO center arrange themselves in close proximity (Fig.8). The suggestion of the existence of an intermediate defect arose from the fact that upon annealing of the 830 cm^{-1} band of VO, and prior

to the emergence of the 887 cm^{-1} band of VO_2, two bands at 914 and 1000 cm^{-1} appeared [19,93] simultaneously in the spectra at intermediate temperatures (Fig.4). Thus, the conversion of VO to VO_2 is more correctly described by the reaction scheme $VO \rightarrow [VO + O_i] \rightarrow VO_2$. The formation process is explained by considering that the Gibbs free energy minimum of the [VO+O_i] defect is intermediate between the respective minima of the VO and VO_2 defects, and, therefore, at the low temperature range of the transition process of VO to VO_2, the formation of the [VO+O_i] structure is potentially likely. The bands at 1000 and 914 cm^{-1} were attributed to the vibrations of the two

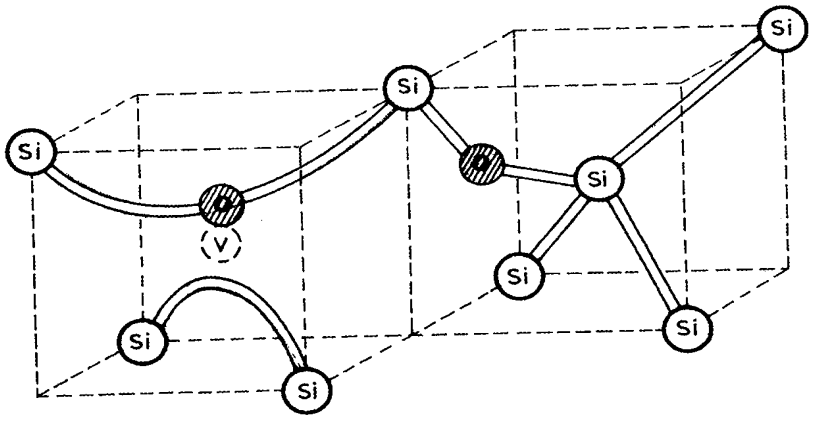

Fig. 8: The configuration of the [VO+O_i] center.

oxygen atoms of O_i and VO parts, respectively, in the [VO+O_i] structure. The LVMs frequencies of the intermediate defect were calculated by considering that the power-law potential given by Eq.20, which describes the oscillations of the oxygen atoms, takes [93] the form:

$$U(r) = \varepsilon\left[\left(\frac{\sigma}{r}\right)^4 - (1 \mp \lambda_{\mp})\left(\frac{\sigma}{r}\right)^2\right] \tag{36}$$

where the $(1-\lambda_-)$ and $(1+\lambda_+)$ factors describe the modifications in the potentials that the O atom of VO and the interstitial oxygen atom see, respectively, in the [VO+O_i] structure. In order to estimate λ_-, λ_+ we have recoursed to the study of the metallicity [89,90,94] of the silicon atom that lies between the two oxygen atoms of the [VO+O_i] structure, and how it is changed by the presence of the oxygen impurity. We found that $\lambda_- = \lambda_+ = 0.075$. The changes of the vibrational frequencies are given [93] by the expression,

$$\frac{\Delta\nu}{\nu_o} = (1 \mp \lambda_{\mp})^{1/2} - 1 \tag{37}$$

On applying this formula, the vibrational frequencies of the [VO+O_i] center were estimated to be 988 and 922cm^{-1} ; these values are in accord with the experimentally detected frequencies at 1000 and 914cm^{-1} respectively.

4.4 VO_3 center

Upon annealing, at about 450°C, the 887 cm^{-1} band begins to decay and three other bands [15,75] at 910, 976 and 1005 cm^{-1} arise simultaneously in the spectra (although another band at 986

cm^{-1} begins to arise at a slightly higher temperature) (Fig.4). The three bands have been attributed to a VO_3 structure formed [75] by the diffusion of VO_2 captured by an oxygen interstitial atom. In the VO_3 defect the third oxygen atom is added adjacent to the VO_2 defect $\left(VO_2 + O_i \equiv VO_3\right)$ (Fig.9). The two oxygen atoms in the initial VO_2 defect are no longer equivalent, giving rise to two LVMs at 976 and 910 cm^{-1}. The oxygen atom of the Si-O-Si-O_i branch vibrates with a frequency of 976 cm^{-1}. The other oxygen atom which is not directly bonded to the Si-O-Si-O_i chain vibrates at 910 cm^{-1}, which is slightly different than that at 887 cm^{-1} of the initial VO_2 core. This is expected, since this atom is

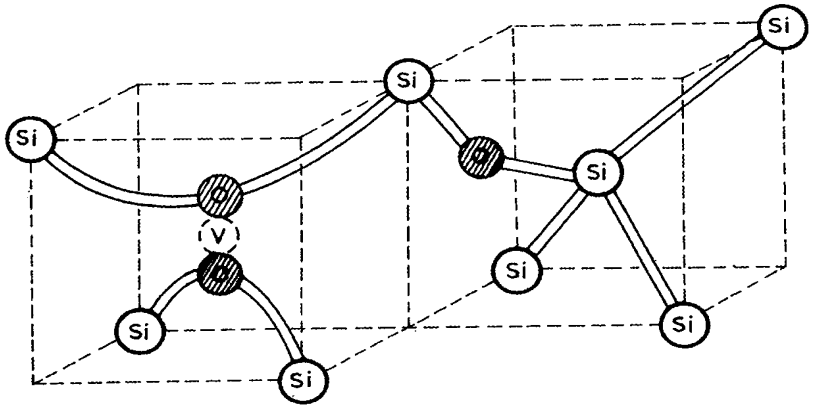

Fig. 9: The configuration of the VO_3 center.

slightly affected by the rest of the atoms of the VO_3 structure. The 1005 cm^{-1} band originates from the vibration of the added O_i that forms a Si-O-Si-O_i chain in the VO_3 structure. Evidently, the assignment of the three bands to a $\left(VO_2 + O_i \equiv VO_3\right)$ structure indirectly supports the assignment of the 887cm^{-1} band to the VO_2 defect. It is worth noting that an isotope experiment which will be expected to verify the number of oxygen atoms in the defect has not yet been reported. The origin of the other LVM at 986 cm^{-1} has not been conclusively identified . It has, however, been tentatively attributed [75] to a modified VO_3 structure with one more oxygen atom attached.

The VO_3 defect has three inequivalent oxygen atoms in its structure and each of them vibrates with a different frequency. For our calculations we shall assume that the VO_3 defect results from a [VO+O_i] defect by the addition of an extra oxygen atom at the vacancy site. The two oxygen atoms that share the same vacant site are not equivalent. Their displacements x_{VO} and x_{VO+O_i} in relation to their equilibrium positions are different for each one of them due to the bonds they make with the rest of the structure. In order to calculate the vibrational frequencies of these two oxygen atoms we use Eq.29 for each one of them separately. We thus have:

$$K' x_{VO} = \frac{2\eta\left(a - x_{VO+O_i}\right)}{4\pi\varepsilon_o\left(a + 2l + \frac{x_{VO} + x_{VO+O_i}}{2}\right)^3}\eta \tag{38}$$

$$K'' x_{VO+O_i} = \frac{2\eta\left(a - x_{VO}\right)}{4\pi\varepsilon_o\left(a + 2l + \frac{x_{VO} + x_{VO+O_i}}{2}\right)^3}\eta \tag{39}$$

where K'' is the force constant of the Si-O bond in the chain Si-O_i-Si-O-Si and K' the corresponding force constant in the chain Si-O-Si. However, due to the general formula $K = m\omega^2$ the following relation holds between K' and K'':

$$\frac{K''}{K'} = \left(\frac{\omega_{VO+O_i}}{\omega_{VO}}\right)^2 \tag{40}$$

In our case $\omega_{VO} = 827cm^{-1}$ and $\omega_{VO+O_i} = 914cm^{-1}$. Since $K' = 92.16\frac{Kgr}{\sec^2}$, as was calculated previously, we finally get $K'' = 112{,}57\frac{Kgr}{\sec^2}$. Upon solving the system of Eqs.38 and 39 for the two unknown parameters x_{VO} and x_{VO+O_i} we get the values: $x_{VO} = 0.08384$ Å and $x_{VO+O_i} = 0.06591$ Å. Consequently, the corresponding relations to Eq.34 for the ω_{VO_3} frequencies of the two oxygen atoms at the same vacant site are:

$$\omega_{1,VO_3} = \omega_{VO}\left(\frac{R_o}{R_{VO}}\right)^3 \frac{1}{2}\left(20\left(\frac{\sigma}{R_{VO}}\right)^2 - 6\right)^{\frac{1}{2}} \tag{41}$$

$$\omega_{2,VO_3} = \omega_{VO+O_i}\left(\frac{R_o}{R_{VO+O_i}}\right)^3 \frac{1}{2}\left(20\left(\frac{\sigma}{R_{VO+O_i}}\right)^2 - 6\right)^{\frac{1}{2}} \tag{42}$$

where $R_{VO} = 1.6341$ Å and $R_{VO+O_i} = 1.6396$ Å are the corresponding lengths estimated according to Eq.35. We finally get:

$$\omega_{1,VO_3} = 901cm^{-1} \text{ and } \omega_{2,VO_3} = 978\,cm^{-1}$$

These values are close to the experimentally observed values, 899 cm^{-1} and 962 cm^{-1} respectively. The frequency ω_{3,VO_3} of the third oxygen atom at the interstitial position is assumed approximately equal to that of O_i in the center [VO+O_i], that is $\omega_{3,VO_3} \approx 1000cm^{-1}$, because the induced changes are negligible for this atom.

The VO_3 defect is generally considered electrical inactive [85], whereas a level at E_c-0.13eV has been tentatively correlated [86] with this defect.

4.5 VO_4 center

Upon annealing at T=520°C the bands of the VO_3 defect anneal out and two new bands at 1032 and 1042 cm^{-1} in neutron irradiated Si appear [19] in the spectra (Fig.4). Within the rationale of the oxygen agglomeration process the two bands were attributed to the $VO_4 \equiv VO_2 + 2O_i$ defect (Fig.10). The addition of an extra oxygen atom to the other leg of the VO_3 defect makes the whole structure symmetric again. Such a complex is expected to give rise to two LVM bands: one originating from the two equivalent oxygen atoms of the VO_2 defect in the core of the VO_4 structure and the other from the other two equivalent oxygen atoms symmetrically located on either side of the VO_2 core, at the legs of the VO_4 structure.

In the case of the VO_4 defect and for our calculations we assume that the defect results from the approach of two [VO+O_i] defects. In order to estimate the vibrational frequency of the two equivalent oxygen atoms that share the same vacant site we are thinking in the same way as we did in the case of the VO_3 center.

Using Eq.29 we have:

$$K''x' = \frac{2\eta(a-x')}{4\pi\varepsilon_o(a+2l+x')^3}\eta \tag{43}$$

whereby we get for x' the value $x' = 0.06868$ Å.

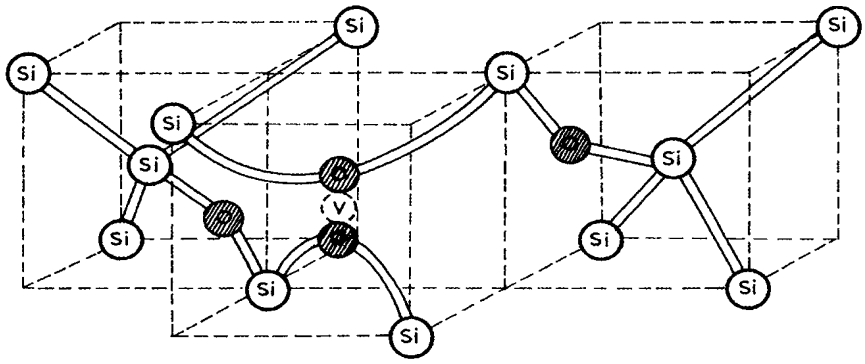

Fig. 10: The configuration of the VO_4 center.

The equation for ω_{1,VO_4} corresponding to Eq.34 is:

$$\omega_{1,VO_4} = \omega_{VO+O_i}\left(\frac{R_o}{R_{VO+O_i}}\right)^3 \frac{1}{2}\left(20\left(\frac{\sigma}{R_{VO+O_i}}\right)^2 - 6\right)^{\frac{1}{2}} \tag{44}$$

Taking into account Eqs.35 and 44 and with $\omega_{[vo+oi]} = 914\ cm^{-1}$ we finally get:

$$\omega_{1,VO_4} = 980\ cm^{-1}$$

The frequencies ω_{2,VO_4} of the other two equivalent interstitial oxygen atoms are considered almost the same as the frequencies of the [VO+O_i] center, that is 1000 cm^{-1}, (since the changes caused are negligible for those atoms).

At this point it is important to note that measurements on oxygen-implanted Si report [95] the emergence of two bands at 1004 and 983 cm^{-1} upon annealing out of the VO_3 defect. These two bands where consequently correlated with the VO_4 defect. In order to explain the absence of these bands in an electron-irradiated material it was argued that the higher concentration of oxygen in the implanted material promotes the addition of O_i making the two bands of VO_4 detectable in the latter case.

Thus, our calculated values of 980 and 1000 cm^{-1} for the frequencies of the VO_4 defect are closer to the experimental values 1004 and 983 cm^{-1} cited in the literature [95] for oxygen implanted Si. However, in our studies, of neutron-irradiated material we have not detected these bands. If the suggestion that the 1004 and 983 cm^{-1} bands are related to the VO_4 defect is correct, then it may be argued that, since above 450°C oxygen interstitials become mobile, it is likely that two oxygen atoms are added sequentially to the VO_2 defect at elevated temperatures $(VO_2 + 2O_i \rightarrow VO_4)$, and therefore the 986 cm^{-1} band, detected in the spectra with some delay in relation with the three bands of VO_3, may be attributed to the VO_4 defect. This is in agreement with a previous suggestion [77] that the 986 cm^{-1} band might arise from a modified VO_3 defect with one more oxygen atoms attached. In this case the other band at 1004 cm^{-1} [95] is rather too weak to be detected and it is only seen in cases of oxygen implantation where the number of the available oxygen atoms becomes

larger. Another way of VO_4 formation may be through oxygen dimers, that is through the reaction $VO_2 + O_2 \rightarrow VO_4$, where an oxygen dimmer is added to a VO_2 defect.

As per the above discussion, one could assume that the 1032 and 1043 cm^{-1} bands in neutron-irradiated Si originate from some unknown oxygen-vacancy clusters. Note, for example, that pentavacancies [96] anneal out at 400-600°C. Also, note that, the oxygen interstitials have become mobile at these temperatures and very mobile oxygen dimers [54] have formed as well. Thus, the 1032 and 1043 cm^{-1} bands may originate from defects formed by multioxygen-multivacancy complexes.

The picture concerning the electrical activity of the VO_4 defect is not clear in the literature. There have been ideas relating the VO_4 center to the core of thermal donors, but definite correlations have not be made [97] so far. The center may be considered as inactive as those of the VO_2 and VO_3 defects. Note, in addition, that the donor behaviour of VO_m centers has been studied theoretically by various methods with conflicting results. There are methods of calculations which confirm [80,98] a donor possibility of VO_m defects although other methods gave negative [99] results.

5. Other oxygen-related centers

5.1 O_i-Si_i centers

Si self-interstitials formed upon irradiation could also pair [100] with O_i. An IR band at ~936 cm^{-1} was attributed [101] to an oxygen interstitial - Si interstitial (O_i-Si_i) center (Fig.11). Although this assignments were later questioned [102], more recent experimental results [103] have verified

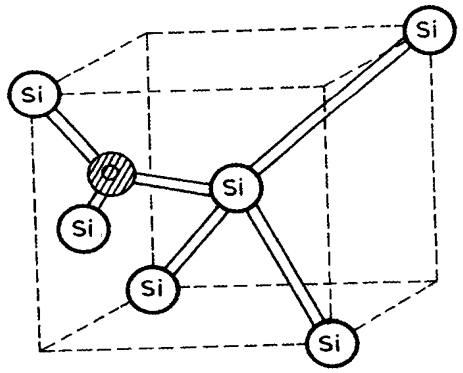

Fig. 11: The configuration of the O_i-Si_i center.

the relation of (O_i-Si_i) center and the 936 cm^{-1} band. The center is unstable and anneals slowly at room temperature. In our studies, where the temperature of irradiation was ~50°C, the annealing was expected to occur during irradiation, and, therefore, any signal from this center was not expected in the spectra. Recent EPR studies [104] have concluded that the (O_i-Si_i) center is a metastable defect. Two EPR spectra labelled Si-AA13 and Si-AA14 were attributed to the positive and negative charge states, respectively, of the one configuration although a spectrum labelled Si-A18 was attributed to the positive charge state of the other configuration.

Complexes of O_i with more than one Si_i have also been put forward. It is worth noting that theoretical studies have suggested [105] that a $Si_i(O_i)_2$ structure is related to the core of thermal

donors. The complex consists of a divalent Si interstitial bonding to an adjacent pair of oxygen interstitials. Two LVMs at 984 and 901 cm^{-1} were estimated , but so far there is no experimental evidence for the defect.

6. V_nO defects

The vacancy aggregation process leading to the formation of V_nO defects is roughly parallel to the oxygen aggregation process leading to the formation of VO_m defects. They differ, however, in some essential respects; for example in the introduction and annealing temperature which is characteristic of each individual defect. In addition, the formation of the more complex defects V_nO_m, to be discussed later, seem to begin [20] from the addition of oxygen atoms or vacancies to the V_nO defects. Among the V_nO complexes, the V_2O and V_3O defects are the main representatives and their vibrational frequencies will be calculated in what follows.

6.1 V_2O center

Early EPR studies [20] have shown that the V_2O defect could form during irradiation of oxygen-rich Si at room temperature, possibly by the successive capture of two isolated vacancies by an oxygen atom. Note, in addition, that during irradiation, divacancies (V2) are also formed. These divacancies become mobile above 200°C and their capture by oxygen atoms provide an alternative channel for the formation of V_2O defects. Above 300°C, where VO become mobile, V_2O could form by the capture of VO pair from oxygen atoms. Analysis of the corresponding A14 EPR spectrum [20] shows that the defect consists of a divacancy and a nearly substitutional oxygen atom trapped near a vacancy site forming a Si-O-Si bond similar to that of the VO defect (Fig.12). This geometry

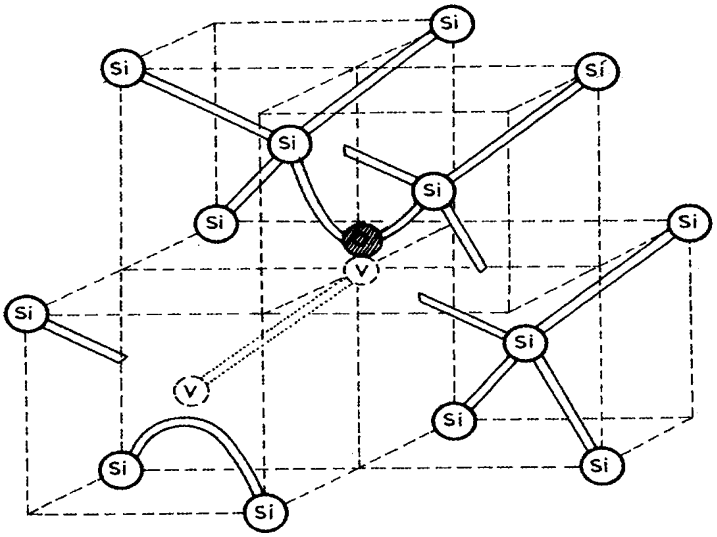

Fig. 12: The configuration of the V_2O center.

has prompted us to calculate [21] the vibrational frequency of the V_2O defect from that of the VO

defect by considering the modification caused in the Si-O-Si bond by the attachment of an extra vacancy next to the Si-O-Si unit of the VO defect. We have considered [88,89] that the oxygen atom in the Si-O-Si bond interacts with the two neighbouring Si atoms with a power law potential described by Eq.20. If K is the force constant of the Si-O bond and R_o its equilibrium length, it can easily be found by putting the derivative $\frac{\partial U}{\partial r}$ equal to zero at $R = R_o$, that $K = \frac{2\varepsilon}{R_o}$.

In a XY_2 molecular model [70] the vibrational frequency of the oxygen atom is given as:

$$\omega_{VO} = \sqrt{\frac{K_{VO}}{m_{Si}}\left(1 + \frac{2m_{Si}}{m_O}\cos^2 \vartheta_{VO}\right)} \tag{45}$$

where ϑ_{VO} is the angle between the <110> axis and the Si-O bond. It is reasonable to assume that a similar relation also holds for the frequency ω_{V_2O} of V_2O defect. Taking into account that $K = \frac{2\varepsilon}{R_o}$ and substituting the ratio of the atom masses m_{Si}, m_O we get:

$$\omega_{V_2O} = \omega_{VO}\frac{R_{o,VO}}{R_{o,V_2O}}\frac{\sqrt{1+3.5\cos^2 \vartheta_{V_2O}}}{\sqrt{1+3.5\cos^2 \vartheta_{VO}}} \tag{46}$$

Using data from an ab-initio calculation analysis [84] we have estimated [21] a frequency ω_{V_2O} equal to 852 cm^{-1}. This value is close to the frequency of the experimentally observed band at 839 cm^{-1} (Fig.13) in the infrared spectra of neutron irradiated Si. Thus, taking in addition into account the

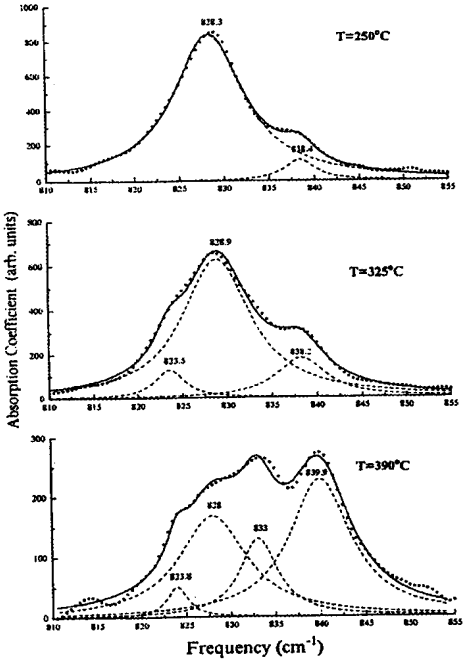

Fig. 13: Deconvolution of the VO center region infrared bands. (ref.[21])

annealing behaviour of this band we have correlated [21] 839 cm^{-1} with the V_2O defect. This is in

agreement with previous studies in electron-irradiated Si, where a band at 835 cm^{-1} has been correlated [18] with the above defect.

The exact electrical activity of the V_2O center is an open question. A number of levels, e.g., at E_c-0.30eV [69], E_c-0.50eV [27] and E_c-0.24eV [106] have been attributed to this defect. The defect is also detected by PAS studies and a lifetime of 270ps have been associated [107] with divacancy-oxygen complexes.

6.2 V_3O center

Upon annealing of the Si-A14 EPR spectrum of the V_2O defect, around 300°C, another spectrum, labelled Si-P4, arises. This spectrum has been attributed [20] to the V_3O defect formed according to the reaction $V_2O + V \rightarrow V_3O$. The geometry of this defect is given in Fig.14. In this

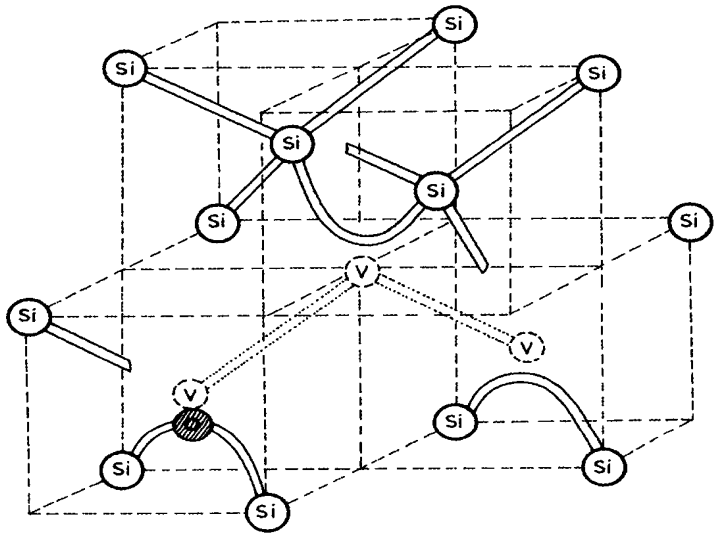

Fig. 14: The configuration of the V_3O center.

geometry an oxygen atom is located in a nearly substitutional site at the end of a three vacancy chain along the <100> axis. The V_3O defect is considered to arise from the V_2O defect by the addition of an extra vacancy. Accordingly, its vibrational frequency could be calculated from that of the V_2O defect by considering the changes in the Si-O bond due to the addition of an extra vacancy. Assuming the oxygen atom to be under the influence of a power potential [88,89] given by Eq.20, we can easily see [108] that the frequency of vibration is inversely proportional on the Si-O bond length R, that is $\omega \propto \frac{1}{R}$. If R_{V_2O} is the Si-O bond length at the equilibrium position in the V_2O structure, where the oxygen atom vibrates with a frequency ω_{V_2O} and R_{V_3O}, ω_{V_3O} are the corresponding parameters for V_3O structure then the relations $\omega_{V_2O} \propto \frac{1}{R_{V_2O}}$, $\omega_{V_3O} \propto \frac{1}{R_{V_3O}}$ lead to the formula:

$$\omega_{V_3O} = \omega_{V_3O} \frac{R_{V_3O}}{R_{V_2O}} \tag{47}$$

The ratio $\frac{R_{V_3O}}{R_{V_2O}}$ has been calculated [107] to be approximately equal to 0.95. Inserting into the above relation this value and with ω_{V_2O} equal to 839 cm^{-1}, i.e. the experimentally detected frequency for V_2O defect, we finally get $\omega_{V_3O} = 883cm^{-1}$. Note that this value is very close to the value of 887 cm^{-1} band attributed to the VO_2 defect.

We recollect, however, what we have already mentioned in paragraph 4.4, that the attribution of the 887 cm^{-1} band to the VO_2 defect only, presents some difficulties, since some experimental data cited in the literature concerning its behaviour could not be reconciled with a VO_2 structure. In our studies [108] the analysis of the 887 cm^{-1} band, using Lorentzian profiles, has shown a small shoulder at 884 cm^{-1} (Fig.15). Thus , we have attributed the 887 cm^{-1} band to the VO_2 defect and 884 cm^{-1} band to the V_3O defect. Such an attribution could explain, for example, the uniaxial stress data. Actually, when two defects are present, the piezospectroscopic tensor obtained provides information [108] about the sum of the piezospectroscopic tensors of these defects and not for each one particular defect. As a consequence of that, the revealed symmetry is lower than that of the higher symmetry defect participant.

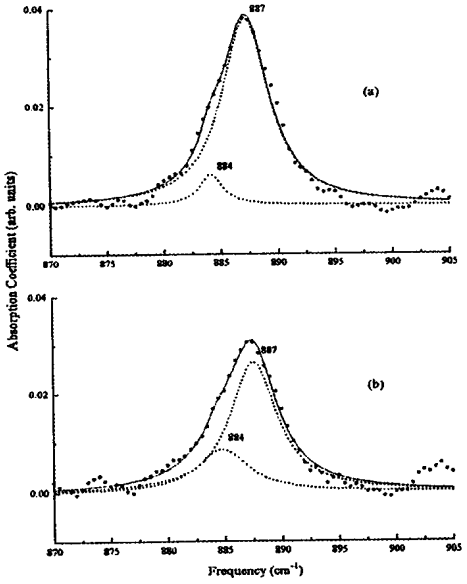

Fig. 15: Deconvolution of the VO_2 center region infrared bands. (ref.[108])

Photo-EPR measurements [27] have correlated an electrical level at E_v-0.40eV to the V_3O defect although DLTS studies [109] have attributed a level at E_v+0.34eV with a capture cross section $\sigma = 2.3 \times 10^{-12} cm^2$. Additionally, a positron lifetime of 325ps has been related [110] to the V_3O defect.

7. V_nO_m defects

Upon annealing at elevated temperatures larger complexes are formed with more than one oxygen atoms and more than one vacancies in their structure. These V_nO_m defects have been mainly detected and studied by the EPR technique. However, there exist LVM bands which could be positively correlated with certain defects as, for example, V_2O_2 and V_3O_2 which will be studied in what follows.

7.1 V_2O_2 center

When the V_2O center becomes mobile, at about 400°C, it either aquires a vacancy to form the V_3O center discussed above or an oxygen atom to form a V_2O_2 complex [20,109]. An EPR spectrum labelled Si-P2 was attributed to the V_2O_2 defect. The geometry of the center is given in Fig.16. It comprises two nearly substitutional oxygen atoms in two neighbouring vacant sites. Its symmetry is C_{2h}. Early IR studies have correlated a LVM band at ~1000 cm^{-1} with V_2O_2 defect mainly by considering the similarities in the annealing behaviour of this defect band and the Si-P2 EPR spectrum.

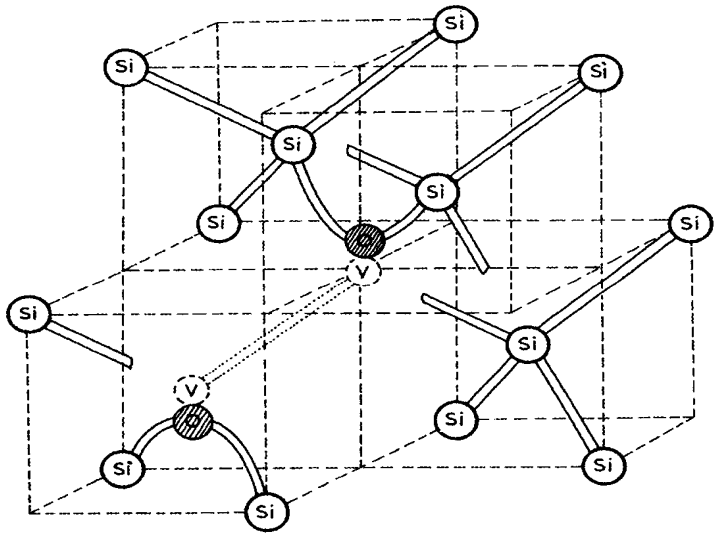

Fig. 16: The configuration of the V_2O_2 center.

As seen from Fig.16 the V_2O_2 defect could be considered as resulting from two VO centers which are coupled together. Prior to attempting to calculate their vibrational frequencies we must note that in any defect where oxygen atoms are not bonded directly and do not occupy second neighboured sites, the interaction between them can be considered as a dipole-dipole moment interaction, since the Si-O bond is a polarised covalent bond. In the case of the V_2O_2 defect the two oxygen atoms can be considered, to a good approximation, as two harmonic oscillators with an interacting potential of the form:

$$W = \frac{\vec{p}_1\vec{p}_2 - 3(\hat{n}\vec{p}_1)(\hat{n}\vec{p}_2)}{d^3} \tag{48}$$

where $\vec{p}_1 = Z^*\left(-r\hat{k} + q_1\hat{q}\right)$ is the dipole moment of the one oxygen atom and $\vec{p}_2 = Z^*\left(r\hat{k} + q_2\hat{q}\right)$ is the dipole moment of the other oxygen atom, Z^* is the effective charge of each oxygen atom, $\hat{k}, \hat{q}$ are the unit vectors along the <001> ,<110> axes, respectively, and d the distance between the dipole moments supposing that they are located on the oxygen site.

Since each oxygen atom vibrates along the <110> axis, in order to estimate the interaction potential, W , we shall take into account only the term of the dipole moment which depends on q. The total Hamiltonian, which describes the motion of the two oxygen atoms of the V_2O_2 defect, is given [21] by the expression

$$H = \frac{1}{2}M_o\dot{q}_1^2 + \frac{1}{2}K_o q_1^2 + \frac{1}{2}M_o\dot{q}_2^2 + \frac{1}{2}K_o q_2^2 + \lambda q_1 q_2 \qquad (49)$$

where $\lambda = \frac{Z^{*2}}{d^3} = 0.3\,eV/\text{Å}^2$ and $K_o = 40.4\,eV/\text{Å}^2$ [21]

Two normal modes are expected to arise from the V_2O_2 defect: i) a symmetric one with frequency $\omega_{sym} = \sqrt{\frac{K_o - \lambda}{M_o}}$ and eigenvector $\frac{q_1 + q_2}{2}$ and ii) an antisymmetric one with frequency $\omega_{antisym} = \sqrt{\frac{K_o + \lambda}{M_o}}$ and eigenvector $\frac{q_1 - q_2}{2}$. In the case of infrared radiation, where the wave length is $\lambda >> 10\,\text{Å}$, only the symmetric normal mode is active and consequently observed in the spectra at the frequency $\omega_{sym} = \sqrt{\frac{K_o - \lambda}{M_o}} = 826cm^{-1}$. Thus, an experimentally observed (Fig.13) LVM band at 824 cm^{-1} has been attributed [21] to V_2O_2 defect. This band arises in the spectra at 320°C as result of the following formation process $VO + VO \rightarrow V_2O_2$.

7.2 V_3O_2 center

The V_3O_2 defect consists of a trivacancy chain [20], where the first and the last vacancy sites are occupied by two oxygen atoms (Fig.17). Considering that the two equivalent oxygen atoms oscillate along the <110> axis, we can proceed by employing the same basic physics as that for the V_2O_2 defect. Thus, the frequencies of the V_3O_2 defect could be derived from the dipole-dipole interaction between the two oxygen atoms, the motion of which is described by an effective Hamiltonian like that of Eq.49. Making use of the fact that in this case $d = 3.8\,\text{Å}$ and $K_o = 40.9\,eV/\text{Å}^2$, the following two LVMs frequencies are found: $\omega_{sym} = 831cm^{-1}$ and $\omega_{anisym} = 837cm^{-1}$. In the case of infrared radiation where the wave length is $\lambda >> 10\,\text{Å}$, only the symmetric normal mode is active and therefore observed in the spectra at the frequency 831 cm^{-1}. Thus, an experimentally observed LVM band at 833 cm^{-1} has been attributed [21] to V_3O_2 defect.

The LVM frequencies of even larger complexes like V_2O_3, V_3O_3, V_4O_2 etc. are expected to have values in the same frequency range. So far, to the best of our knowledge, any correlation of certain LVM bands with the above defects does not exist in the literature, although their presence by other experimental techniques has been definitely verified [20,22] in oxygen-rich materials. Thus, it does not seem prudent to try to estimate these frequencies. As we have already mentioned, multivacancies (V_2 up to V_5) are always present in Si [23]. In addition, recent calculations suggest that larger vacancy aggregates [111], as for example V_6, may be particularly stable configurations. Similar suggestions exist for even larger clusters like V_{10}, V_{14}, etc. [112]. It seems likely, therefore,

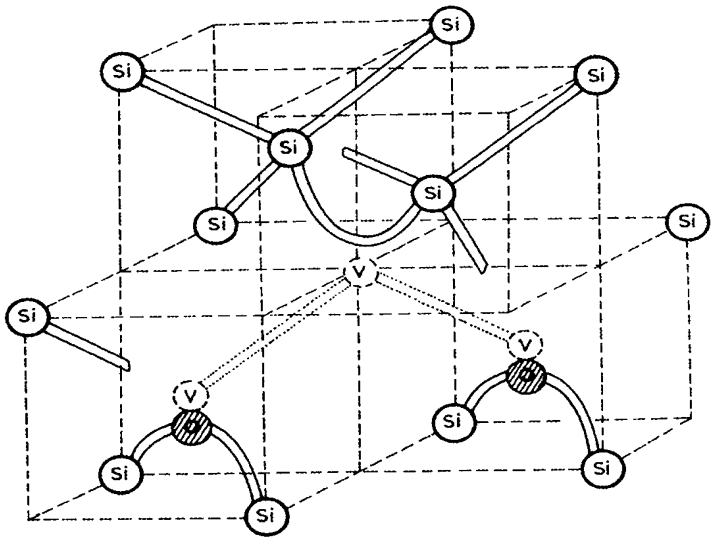

Fig. 17: The configuration of the V_3O_2 center.

in Cz-Si that large vacancy clusters probably form containing oxygen atoms. The full understanding of these large clusters needs further investigation both theoretical and experimental.

SUMMARY

In this paper, the present knowledge of the oxygen vacancy (V_nO_m) defects have been reviewed. The fundamental aspects concerning the structural properties of these defects have been discussed. A compilation of results from experimental techniques, for example DLTS, PAS, and especially EPR have been cited and discussed in relation to experimental data obtained by IR spectroscopy. Subsequently, theoretical calculations have been conducted for the purpose of linking LVMs to defects structure.

IR spectroscopy is an important experimental technique for the study of defects in solids and it has been used extensively in the field of semiconductors. The defects are detected due to their LVMs, even if they do not introduce states into the energy gap or they do not have an unpaired electron as required for their detection by the DLTS and EPR techniques, respectively. In addition, LVM bands and their behaviour to external perturbations like stresses, polarised light and isotope substitution provide adequate information necessary for determining the chemical nature and the physical structure of a defect, that is the identity of the defect.

Oxygen is the most important impurity in Si. Although, a large body of information is available about its complexing with lattice vacancies to form V_nO_m defects, a clear picture for some of them has not emerged so far. Definite correlations, for example, of a number of experimentally observed LVMs with certain V_nO_m defects do not exist. To this end, we reviewed the structural properties of the various V_nO_m defects in Cz-Si, employing at the same time semiempirical calculations to estimate the vibrational frequencies of these defects. In particular, we have been engaged in studying the serial formation of VO_m, V_nO and the evolution of V_nO_m defects. The LVM frequencies of VO, [VO+ O_i], VO_2, VO_3, VO_4, V_2O, V_3O, V_2O_2, V_3O_2 defects have been confirmed.

An important point we discussed is the existence of a shoulder (Fig.15) in the frequency range of the VO_2 defect. The attribution of this shoulder to the V_3O defect provides help for understanding uniaxial stress data concerning the behaviour of the 887 cm^{-1} band in Si. Another interesting point has to do with the correct band assignments of the VO_4 defect. Between two pairs of frequencies cited in the literature, as linked to VO_4 defect, that is the pairs 986, 1004 cm^{-1} and 1032, 1043 cm^{-1}, our calculations point to the former one as the most likely candidate. If this assignment is confirmed, then the origin of the latter pair of bands has yet to be established. The LVM frequencies of large V_nO_m complexes, as for example V_3O_3, V_4O_2, V_4O_3 etc., which have been seen by EPR or PAS techniques, has not been determined so far mostly because their IR signals are expected to be very weak. Thus, experimental and theoretical work concerning their LVMs bands remains to be done.

In any case, the present knowledge of the V_nO_m defects is at a very advanced level and the picture tends to be more or less sufficiently clear. In this, the contribution of IR spectroscopy is undoubtedly significant.

REFERENCES

[1] R.C.Newman , Rep. Prog.Phys. 45 (1982), p.1163
[2] A.Borghesi, B.Pivac, A.Sassella and A.Stella, J.Appl.Phys. 77 (1995), p.4169.
[3] S.M.Hu and W.J. Petrick, J. Appl. Phys 46 (1975) , p.1869
[4] T.Y. Tan, E.E. Gardner and W.K. Tice, Appl. Phys. Lett. 30 (1977) , p.175
[5] R.C. Newman, Mat. Res. Soc. Symp Proc. 104 (1988) , p.25
[6] B. Pajot, in Semiconductors and Semimetals, edit.F.Shimura, Academic Press, vol. 42, Chapter 6 (1994) , p. 191
[7] H.Bender and J.Vanhellemont, in Handbook on Semiconductors, (edit. by Mahajan, Elsevier, North Holland), Vol.3b (1994), p.1637
[8] W.C. O'Mara, in Handbook of Semiconductor Silicon Technology (edit. by W.C.O'Mara, R.B.Herring and L.P.Hunt, Noyes Publications) chapter 7 (1992) , p.451
[9] J.W.Corbett and J.C.Bourgoin, in Point Defects in Solids vol.2 , Semiconductors and Molecular crystals (edit. J.H.Craword and L.M.Slifkin, Plenum Press New York) (1975), p.1
[10] G.D Watkins and J.W. Corbett Phys. Rev. A 138 (1965) , p.543
[11] J.W. Corbett and G.D. Watkins Phys. Rev. A 138 (1965) , p.555
[12] Y.H. Lee, N.N. Gerasimenko and J.W. Corbett , Phys. Rev.B14 (1976), p.4506
[13] H. Stein, in 2nd International Conference of Neutron Transmutation Doping in Semiconductors, edited by J.M. Meese (Plenum New York, 1979) p.229
[14] G.D. Watkins and J.W Corbett Phys. Rev. 121 (1961) ,p.1001
[15] J.W Corbett, G.D. Watkins, R.M. Chrenko and R.S.Mc Doland Phys. Rev. 121 (1961) , p.1015
[16] H.J. Stein, Rad. Effects 22 (1974) , p.169
[17] J.W Corbett, G.D. Watkins and R.S.Mc Doland, Phys. Rev. 135 A (1964) , p.1381
[18] Y.H. Lee, J.C. Corelli and J.W. Corbett, Phys. Lett. 60A (1977) , p.55
[19] C.A. Londos, G.I. Georgiou, L.G. Fytros, and K.Papastergiou, Phys.Rev.B 50 (1994) , p.11531
[20] Y.H. Lee and J.W Corbett, Phys. Rev. B13 (1976) , p.2653
[21] N.V. Sarlis, C.A. Londos and L.G. Fytros J. Appl. Phys. 81 (1997) , p.1645
[22] A.Li, H.Huang, D.Li, S.Zheng, H.Du, S.Zhu and T.Iwata, Jpn.J.Appl.Phys. 32 (1993) , p.1033
[23] Y.H.Lee and J.W.Corbett, Phys.Rev. 8, 2810 (1973); and S.J. Pearton, J.W Corbett and M. Stavola, Hydrogen in Crystalline Semicoductors, edited by H.J. Quisser, (Springer-Verlong Berlin, 1992) p.180

[24] A.V. Druvechenskii, A.A. Karanovich and V.V. Suprunchik, Rad. Eff. Def. Sol. Vols 111 and 112 (1989) , p.91
[25] P.Asoka-Kumar, K.G. Lynn and D.O. Welch J. Appl. Phys. 76 (1994) , p.4935
[26] P. Mascher, S. Dannefaer and D. Kerr Mat. Sci. Forum Vol. 38-41 (1989) , p.1157
[27] Y.H.Lee, T.D.Bilash and J.W.Corbett, Rad.Effects 29 (1976) , p.7
[28] L.C.Kimerling, Inter. Conf. on Radiation Defects in Semiconductors, Dubrovnic 1976, Inst. Phys. Conf. Ser. no 31, edit. by N.B.Urli and J.W.Corbett (IOP, Bristol, 1977) p. 221
[29] Yu.M.Dobrovinskil, Sh.Makhkamov, A.Mirraev, V.I.Mitin and N.A. Tursunov, Sov.Phys.Semicond. 25 (1991) , p.316
[30] C.Cohen-Tannoudji, J.Dupont-Roc and G.Grynberg, Photons and Atoms, Introduction to Quantum Electrodynamics (edit. J.Wiley and sons, New York 1989)
[31] J.D.Jackson, Classical Electrodynamics, J.Wiley & Sons, New York (1962)
[32] R.C. Newman, Infrared studies of crystal defects, (Taylor and Fransis, London) (1973)
[33] A.S.Barker Jr and A.J.Sievers, Rev.Modern Physics 47, suppl.2 (1975)
[34] M.Lanoo and J.Bourgoin, Point Defects in Semiconductors I, Springer Ser. Solids-State Sci. vol.22 (Springer, Berlin, Heidelberg 1981)
[35] W.Kaiser, P.H. Keck and C.F. Lange Phys. Rev. 101 (1956) , p.1264
[36] V. Takano and M. Maki, in Semiconductor silikon (1973) (Ed. H.R. Huff and RR. Burgess, Electrochemical Society, Penigton, N.J) p.469
[37] D.R. Bosomworth, W. Hayes, A.R.L. Spray and G.D. Watkins, Proc. Poy. Soc. London A 317 (1970) , p.133
[38] B. Pajot and B. Cales, Mat. Res. Sol. Symp Proc. 59 (1986) , p.39
[39] American Institute of Physics Handbook, 3rd ed. (MC Grow- Hill, New York, 1972)
[40] W.C.O'Mara, in Defects in silicon (1983) (ed. W.M. Bulis and L.X. Kimerling, Electrochemical society, Pennigton, NJ) p.120
[41] H.J. Hrostowski and R.H. Kaiser Phys. Rev. 107 (1957) , p.966
[42] R.M. Chrenko, R.S. Mc Doland and E.M. Pell, Phys. Rev. A 138 (1965) , p.1775
[43] J. F. Angress, A.R. Goodwin and S. D. Smith Proc. Roy. Soc. A 308 (1968) , p.111
[44] T. Hallberg, L.I. Murin, J.L. Lindstrom and V.P. Markevich,J. Appl. Phys. 84 (1998) , p.2466
[45] B. Pajot, in Proceedings of the NATO Advanced Workshop on the Early Stages of Oxygen Precipitation in Silicon, Exeter UK ed R. Jones, NATO ASI series 3, High technology (Kluwer Academic, Dordrecht 1996) Vol. 17 (1996), p.283
[46] H. Yamada-Kaneta, C. Kaneta and T. Ogawa, Phys. Rev. B42 (1990) , p.9650
[47] E. Artacho, A. Lizou-Nordstrom and F. Yudurain, Phys. Rev. B51 (1995) , p.7862
[48] E. Artacho, F. Yudurain, B. Pajot, R. Ramirez, C.P. Herrero, L.I. Khirunenko, K.M. Itoh and E.E. Haller, Phys. Rev. 56 (1997) , p.3820
[49] J. Wagner, K.Thonke and R. Sauer Phys. Rev. B 29 (1984) , p.7051
[50] L. Ohkoshi, J. Phys. C 18, (1985) p.5415
[51] C.S. Fuller, J.A. Ditzenberger, N.B. Hannay and E. Buhler Phys. Rev. A 96 (1954) , p.833
[52] W. Kaiser and P. Keck, J.Appl.Phys. 50 (1957) , p.8095
[53] P.Wagner and J.Hage, J.Appl.Phys. A49 (1989) , p.123 ; and W.Gotz, G.Pensl and W.Zulehnev, Phys.Rev. B46 (1992) p.4312.
[54] R.C.Newman, Proc. 20th Inter. Conf. Defects in Semiconductors edit by E.M.Anastassakis and J.D.Ioannopoulos (World Scientific, Singapure 1990) p.525
[55] J.L.Lindstrom and T.Hallberg, Phys. Rev. Lett. 72, 2729 (1994), and J.Appl.Phys. 77 (1995) , p.2684
[56] U.Gosele, K.Y.Ahn, B.P.R.Morioton, T.Y.Tan and S.T.Lee, Appl. Phys. A 48 (1989) , p.219
[57] S.A.McQuaid, M.J.Binns, C.A.Londos, J.H.Tucker, A.R.Brown and R.C.Newman, J.Appl.Phys. 77 (1995) , p.1427
[58] U.Gosele and T.Y.Tan, Appl. Phys. A 28 (1982) , p.79

[59] R.C.Newman and R.Jones, Semiconductors and Semimetals, vol. 42 (1994) , p.289
[60] L.C.Snyder, J.W.Corbett, P.Deak and R.Wu, Mater.Res.Soc.Symp.Proc. 104 (1988), p.179
[61] L.I.Murin, T.Hellberg, V.P.Markevich and J.L.Lindstrom, Phys.Rev.Lett. 80 (1998), p.93
[62] K.Tempelhoff, F.Spielberg, R.Gleichmann and D.Wruck, phys.stat.sol.(a) 56 (1979), p.213.
[63] M.Hu, J.Appl.Phys. 51 (1980), p.5945.
[64] G.D. Watkins, J.W. Corbett, R.M. Walker J. App. Phys. 30 (1959) , p.1198
[65] H.Y. Fan and A.K. Ramdas, Proc. Int. Conf. Semicond. Physics, Prague, Czech Acad. Sci. (1961) p.309
[66] A.R. Bean and R.C. Newman Solid State Commun. 9 (1971) , p.271
[67] K.L. Brower Phys.Rev., B4 (1970) , p.1968
[68] G.K. Wertheim, Phys.Rev. 121 (1957) , p.1001
[69] L.C. Kimerling, in Radiation Effects in Semiconductors, eds N.B. Urli and J.W. Corbett (IOP, London 1977) p. 221
[70] G.Herzberg, Molecular Spectra and Molecular Structure, Vol.2, Infrared and Raman Spectra of Polyatomic Molecules, (Van Nostrand-Reinhold, New York, 1945)
[71] M.T.Lappo and V.D.Tkachev, Sov.Phys.Semicond. 4 (1970) , p.418
[72] H. J. Stein and F.L. Vook, Appl. Phys. Lett. 13 (1968), p.343
[73] H.J. Stein and F.L. Vook, Rad. Effect. 1 (1969) , p.41
[74] R.C. Newman, A.S. Oates and F. M. Lirington, J. Phys. C: Solid State Physics, 16 L (1983), p.667
[75] B.G. Svenson and J.L. Lindstrom Phys. Rev. B 35 (1986) , p.8709
[76] C.A. Londos, N.V. Sarlis and L.G. Fytros, phys. stat. sol. (a) 163 (1997) , p.325
[77] J.L. Lindstrom and B.G. Svenson, Mat. Res. Soc. Symp. Proc. 59 (1986) , p.45
[78] R.C. Newman and R.Jones, Semiconductors and Semimetals, edit. by F.Shimura, Academic Press vol.42, chapt. 8 (1994) , p.289
[79] H.J. Stein, Appl. Phys. Lett. 48 (1986) , p.1540
[80] G.G. Deleo, C.S. Milsted, Jr and J.C. Kvalik, Phys. Rev. B. 31 (1985) , p.3588
[81] H.J. Stein, Mater. Sci. Form 10-12 (1986) , p.935
[82] K.N. Andreerskil and B.M. Trakhbrot, Sov. Phys. Semicond. 24 (1991) , p.1325
[83] C.P. Ewels, R. Jones and S. Oberg, Mater Sci. Forum vol. 196-201 (1995) , p.1297
[84] W.W.Keller, J.Appl.Phys. 55 (1984) , p.3471
[85] J. Svenson, B.G. Svenson and J.L. Lindstrom Appl. Phys. Let. 49 (1986) , p.1435
[86] Y.M. Dohrovinskil, S. Mokhkamor, A. Mirzaer V.L. Mitin and N.A. Tursunov, Sov. Phys. Semicond 25 (1991) , p.316
[87] S. Dannefaer, Phys. Sat. Sol. (a) 102 (1987) , p.481
[88] W.Harrison, Electronic structure and the properties of solids (Dover, N.York, 1989)
[89] W.Harrison, Phys.Rev.B, 27 (1983) , p.3592
[90] S.Pantelides and W.Harrison, Phys.Rev.B 13 (1976) , p.2667
[91] P. Deak, Material Science Forum, 38-41 (1989) p.281
[92] Y.V.Pomozov, L.I.Khirunenko, V.I.Shakhotsov and V.I.Yashnik, Sov. Phys. Semicond. 24 (1990), p.624
[93] C.A. Londos, N. Sarlis, L.G. Fytros and K. Papastergiou Phys. Rev. B 53 (1996) , p.6900
[94] S. Pantelides and W. Harrison Phys. Rev. B 11 (1975) , p.3006
[95] H.J.Stein, in Defects in Semiconductors edit. by H.J.Von Bardeleben, Mater.Sci.Forum vols 10-12 (1986) , p.935
[96] L.Sealy, R.C.Barklie, W.L.Brown and D.C.Jacobson, Nucl. Instrum. Methods Phys. Res. 80/81 (1993) , p.528
[97] D.J.Chadi, Phys.Rev.B 41 (1990) , p.10595
[98] G.G.Deleo, W.B.Fowler and G.D.Watkins, Phys.Rev.B 29 (1984) , p.3193
[99] P.J.Kelly, Mater.Sci.Forum 38-41 (1989) , p.269

[100] R.D.Harris and G.D.Watkins, Proc 13th Int.Conf. defects in Semiconductors, edit. by L.C.Kimerling, J.J.Parsey Jr., Coronado (AIME: New York) (1985) , p.799
[101] A.Brelot, in Radiation Damage and Defects in Semiconductors, edit. by J.Whitehouse, Institute of Phys. London (1973), p.191
[102] J.L.Lindstrom, B.G.Svenson, J.W.Corbett and G.S.Oehrlein, phys.stat.sol. (a) 85,K (1984), p.109
[103] H.J.Stein, Appl.Phys.Lett. 55 (1989) , p.870
[104] K.A.Abdullin, B.N.Mukashev, A.M.Makhov and Y.V.Gorelkinskii, Mat.Sci. Engineering B36 (1996) , p.77
[105] P.Deak, L.C.Snyder and J.W.Corbett, Phys.Rev.Lett. 66 (1991) , p.747
[106] M.A.Trauwaert , J.Vanhellemont, H.E.Maes, A.M.VanBavel, G.Langouche and P.Clauws, Appl.Phys.Lett. 66 (1995) , p.3057
[107] P.Mascher, S.Dannefaer and D.Kerr, Phys.Rev.B 40 (1989) , p.11764
[108] C.A. Londos, N.V. Sarlis and L.G. Fytros, J.Appl.Phys. to be published
[109] T.Maekawa, S.Inone and A.Usami, Semicon. Sci. Technol. 5 (1990) , p.663
[110] A.Kawasuso, M.Hasegawa, M.Suezawa, S.Yamaguchi and K.Sumino, Appl.Surf.Sci. 85 (1995) , p.280
[111]J.L.Hastings, S.K.Estreicher and P.A.Fedders, Phys.Rev.B 56 (1997) , p.10215
[112]D.J.Chadi and K.J.Chang, Phys.Rev.B 38 (1998) , p.1523